

1  
2  
3  
4

**TITLE PAGE**  
**- Korean Journal for Food Science of Animal Resources -**  
**Upload this completed form to website with submission**

ARTICLE INFORMATION	Fill in information in each box below
<b>Article Type</b>	Research article
<b>Article Title</b>	Effect of postmortem phases on lamb meat quality: A physicochemical, microstructural and water mobility approach
<b>Running Title (within 10 words)</b>	Effect of postmortem phases on lamb meat quality and microstructure
<b>Author</b>	Yue Ge, Dequan Zhang, Huimin Zhang, Xin Li, Fei Fang, Ce Liang, Zhenyu Wang*
<b>Affiliation</b>	Institute of Food Science and Technology, Chinese Academy of Agricultural Sciences, Key Laboratory of Agro-products Quality and Safety Control in Storage and Transport Process, Ministry of Agriculture and Rural Affairs, Beijing, 100193, P. R. China
<b>Special remarks – if authors have additional information to inform the editorial office</b>	
<b>ORCID (All authors must have ORCID) <a href="https://orcid.org">https://orcid.org</a></b>	Yue Ge ( <a href="https://orcid.org/0000-0002-0214-9541">https://orcid.org/0000-0002-0214-9541</a> ) Dequan Zhang ( <a href="https://orcid.org/0000-0003-3277-6113">https://orcid.org/0000-0003-3277-6113</a> ) Huimin Zhang ( <a href="https://orcid.org/0000-0002-3713-0656">https://orcid.org/0000-0002-3713-0656</a> ) Xin Li ( <a href="https://orcid.org/0000-0001-7924-6449">https://orcid.org/0000-0001-7924-6449</a> ) Fei Fang ( <a href="https://orcid.org/0000-0001-6640-804X">https://orcid.org/0000-0001-6640-804X</a> ) Ce Liang ( <a href="https://orcid.org/0000-0003-2859-2610">https://orcid.org/0000-0003-2859-2610</a> ) Zhenyu Wang ( <a href="https://orcid.org/0000-0003-4478-1710">https://orcid.org/0000-0003-4478-1710</a> )
<b>Conflicts of interest</b> List any present or potential conflict s of interest for all authors. (This field may be published.)	The authors declare no potential conflict of interest.
<b>Acknowledgements</b> State funding sources (grants, funding sources, equipment, and supplies). Include name and number of grant if available. (This field may be published.)	This research was financially supported by the Agriculture Research System (CARS-38), Key Research and Development Plan Project of Hebei Province (19227121D), and National Agricultural Science and Technology Innovation Program (CAAS-ASTIP-2020-IFST) in China.
<b>Author contributions</b> (This field may be published.)	Conceptualization: Zhenyu Wang, Dequan Zhang. Data curation: Yue Ge, Huimin Zhang, Zhenyu Wang, Dequan Zhang. Formal analysis: Xin Li. Methodology: Yue Ge, Fei Fang, Ce Liang. Software: Yue Ge. Validation: Yue Ge. Investigation: Yue Ge, Huimin Zhang,Ce Liang. Writing - original draft: Yue Ge. Writing - review & editing: Zhenyu Wang, Xin Li, Fei Fang, Dequan Zhang. (This field must list all authors)
<b>Ethics approval (IRB/IACUC)</b>	This manuscript does not require IRB/IACUC approval because there

(This field may be published.)	are no human and animal participants.
--------------------------------	---------------------------------------

5

6 **CORRESPONDING AUTHOR CONTACT INFORMATION**

<b>For the <u>corresponding</u> author (responsible for correspondence, proofreading, and reprints)</b>	<b>Fill in information in each box below</b>
First name, middle initial, last name	Zhenyu Wang
Email address – this is where your proofs will be sent	caasjgsmeat2021_1@126.com
Secondary Email address	wangzhenyu@caas.cn
Postal address	Institute of Food Science and Technology, Chinese Academy of Agricultural Sciences, No. 2 Yuanmingyuan West Road, Haidian District, Beijing, 100193, P. R. China.
Cell phone number	
Office phone number	Tel: +86-10-62818740
Fax number	Tel: +86-10-62818740

7

8

9

ACCEPTED

---

10                   **Effect of postmortem phases on lamb meat quality: A**  
11                   **physicochemical, microstructural and water mobility approach**

12   **Abstract**

13           To investigate the effect of postmortem phases on lamb meat quality, the  
14   physicochemical quality, microstructure and water mobility of oyster cut, short loin,  
15   knuckle and silverside muscles from Small-Tail Han sheep were evaluated in the  
16   pre-rigor, rigor mortis and post-rigor phases. Pre-rigor lamb meat had higher pH and  
17   water holding capacity, whereas lower CIE L\*, b\*, hue angle values than rigor mortis  
18   and post-rigor meat ( $p < 0.05$ ). The Warner-Bratzler shear force values were higher in  
19   rigor mortis short loin and silverside than their pre-rigor and post-rigor counterparts,  
20   pre-rigor short loin had lower Warner-Bratzler shear force value than its post-rigor  
21   counterpart ( $p < 0.05$ ). Muscle fibers shrank laterally and longitudinally during the  
22   onset of rigor mortis. Rigor mortis and post-rigor lamb meat exhibited wide I-bands,  
23   dark A-bands, short sarcomeres and large inter-myofibrillar spaces. The shift of  
24   immobilized water to free water and repulsion from the intra-myofibrillar space to the  
25   extracellular space result in the increase of water loss in rigor mortis and post-rigor  
26   lamb meat. The results of the principal component analysis (PCA) indicated that rigor  
27   mortis and post-rigor lamb meat had similar quality properties but different from  
28   pre-rigor lamb meat. In conclusion, the lamb meat in the pre-rigor phase had good  
29   tenderness, color and water holding capacity. The results of this research could  
30   provide some theoretical references for lamb meat production and processing.

31   **Keywords:** lamb meat quality, pre-rigor, rigor mortis, post-rigor, microstructure

---

## 1. Introduction

Lamb meat is one of the most popular meat in many countries of the world, and the consumption of lamb meat is increasing globally (Suleman et al., 2020). The consumption patterns of lamb meat are very diverse in different regions around the world (Nam et al., 2010). In the U.S., Australia and other Western places, the commercial abattoirs commonly use chilling procedure to produce aged lamb meat, with aging time commonly from 5 to 28 days and even longer (Colle et al., 2016; Geesink et al., 2011; Kim et al., 2018; Xiao et al., 2020). However, consumers in some Eastern countries, such as China, prefer pre-rigor meat, which is ubiquitous in Chinese commercial abattoirs (Xiao et al., 2020). Without aging process, pre-rigor meat requires less cooler space, electricity consumption and capital investment (Lang et al., 2016; Sukumaran et al., 2018).

The conversion of muscle to meat and subsequent aging involve complex energy metabolism, biochemical and physiological changes, including the pre-rigor, rigor mortis and post-rigor phases (Lawrie and Ledward, 2017; Xiao et al., 2020). Generally, the pH of lamb muscle declines to ultimate pH at 24 h postmortem, with the muscle fibers enter rigor and the muscle stiffness occurs, complete rigor mortis was attained (Lawrie and Ledward, 2017). During subsequent aging process, with the degradation of cytoskeletal proteins and the increase of sarcomere length, the muscle tension decreased (resolution of rigor mortis) (Lawrie and Ledward, 2017). Xiao et al. (2020) reported that before 12 h postmortem the lamb topside muscle was in the pre-rigor phase, 12-24 h postmortem was in the rigor mortis phase, 3-7 days

---

54 postmortem was in the post-rigor phase according to the pH and Warner-Bratzler  
55 shear force (WBSF) values.

56 The process of rigor mortis and resolution of muscle could affect the meat  
57 quality significantly (Lawrie and Ledward, 2017; Xiao et al., 2020). Wheeler and  
58 Koohmaraie (1994) reported that the WBSF of ovine *longissimus* muscle increased  
59 from 5.10 kg at 3 h postmortem (per-rigor) to 8.66 kg at 24 h postmortem (rigor  
60 mortis), and then decreased to 4.36 kg by 72 h postmortem (post-rigor). Wu et al.  
61 (1995) found that pre-rigor bovine *stemomandibularis* muscle was more tender than  
62 post-rigor control muscle cooked to 70°C internally. The amount of free water  
63 increased during rigor mortis and resolution, which caused an accumulation of water  
64 on the cut surface and higher drip loss (Devine et al., 2014). Meat tenderness, color  
65 and water holding capacity (WHC) are main quality traits concerned by consumers  
66 and meat industry (Li et al., 2020). To date, the quality properties of rigor mortis and  
67 post-rigor meat have been systematically investigated (Colle et al., 2016; Lawrie and  
68 Ledward, 2017; Pearce et al., 2011). However, little is known about the quality  
69 properties of per-rigor lamb meat. Therefore, the aim of this research was to  
70 investigate the physicochemical quality and microstructure of pre-rigor (45 min  
71 postmortem), rigor mortis (24 h postmortem) and post-rigor (72 h postmortem) lamb  
72 meat, and the principal component analysis (PCA) method were used to compare and  
73 analyze the differences of quality properties of lamb meat in different stages of  
74 postmortem.

## 75 2. Materials and methods

---

## 76 2.1 Animals and cuts collection

77 Fifty-four male sheep carcasses (8 months of age, Small-Tail Han sheep) with  
78 the same feeding system (drylot feeding with the same commercial diet) were  
79 randomly collected at a local commercial abattoir in Hebei, China. The Small-Tail  
80 Han sheep is a predominant local sheep variety and widely raised in many provinces  
81 of China, which originated from Mongolia Sheep and carefully cultivated for a long  
82 time in northern China (Li et al., 2018). The 54 carcasses were allocated randomly to  
83 three groups for sampling in pre-rigor (45 min postmortem), rigor mortis (24 h  
84 postmortem) and post-rigor (72 h postmortem) with 18 carcasses in each group. All of  
85 the carcasses were hot-deboned, about 200 g of meat sample was obtained from the  
86 oyster cut (a mixture of *subscapularis*, *infraspinatus*, *teres minor* and *supraspinatus*),  
87 short loin (*longissimus thoracis et lumborum*), knuckle (*quadriceps femoris*) and  
88 silverside (a mixture of *biceps femoris* and *semitendinosus*) in the right side of the  
89 lamb carcasses immediately after slaughter. After trimming the external fat and  
90 connective tissue, each sample was dissected into two sections. One section was  
91 wrapped in polyethylene cling film and placed in a chiller (~4°C) used for pH, color  
92 and microstructure analysis; the other section was vacuum packed (the average  
93 packaged weight was 128.63±8.28 g), frozen (at 45 min postmortem or after  
94 refrigerating at 4°C for 24 or 72 h) and stored at -35°C for further WHC and WBSF  
95 measurements.

## 96 2.2 pH measurement

97 The pH measurement was performed using a portable pH meter (Testo 205, Testo,

---

98 Lenzkirch, Germany). The glass probe of the pH meter was directly inserted into the  
99 center of the samples after calibrating with pH 4.00 and pH 7.00 standard buffers. For  
100 each sample, four measurements were made at different positions, and the average  
101 value was used for further analysis.

## 102 2.3 Color measurement

103 The cut surface was exposed in the air for 30-40 min at ~4 °C to allow blooming  
104 prior to color determination. The color analysis was conducted by a portable  
105 colorimeter (Minolta CR-400, Konica Minolta Optics, Inc.) according to Calnan et al.  
106 (2016). The lightness (CIE L\*), redness (CIE a\*) and yellowness (CIE b\*) of the  
107 samples were recorded, and the parameters hue angle and Chroma were calculated by  
108 the equations  $\tan^{-1}(b^*/a^*)$  and  $\sqrt{a^{*2} + b^{*2}}$ , respectively.

## 109 2.4 Water holding capacity (WHC) analysis

### 110 2.4.1 Thawing loss

111 Frozen samples (128.63±8.28 g) were thawed at 4°C for 16 h, thawing loss was  
112 expressed as a percentage of weight loss before and after thawing (Li et al., 2012).

### 113 2.4.2 Cooking loss and total moisture loss

114 The cooking loss of the samples was determined according to the procedure  
115 described by Hopkins et al. (2010). Briefly, thawed samples were dissected into  
116 blocks with the weight of 65 g, placed inside polyethylene bags and cooked for 35  
117 min in 71°C water-bath. Cooking loss was expressed as a percentage of weight loss  
118 before and after cooking. Total moisture loss was the sum of thawing loss and cooking

---

119 loss.

### 120 2.4.3 Low-field nuclear magnetic resonance (LF-NMR) analysis

121 <sup>1</sup>H NMR transverse relaxation times ( $T_{2b}$ ,  $T_{21}$ ,  $T_{22}$ ) and their corresponding water  
122 populations ( $P_{2b}$ ,  $P_{21}$ ,  $P_{22}$ ) measurements were conducted on an NMR analyzer  
123 (NM120-040H-1, Niumag Electric Corporation, Shanghai, China) by using the  
124 Carr-Purcell-Meiboom-Gill (CPMG) sequences (Li et al., 2014). After thawed at 4°C  
125 for 16 h, the samples were cut into  $3 \times 1 \times 1$  cm parallel to the orientation of muscle  
126 fiber, placed in a plastic tube and inserted into the NMR probe. The analysis was  
127 performed at 32°C. The spectrometer frequency was 20 MHz, and the  $\tau$  value (time  
128 between 90° pulse and 180° pulse) was 100  $\mu$ s. The repetition time between the two  
129 succeeding scans was 1,500 ms. Data were acquired as 8 scan repetitions for each  
130 sample. The data were expressed by using the software of MultiExp Invert Analysis  
131 4.6 (Niumag Electric Corporation, Shanghai, China).

### 132 2.5 Warner-Bratzler shear force (WBSF) measurement

133 The WBSF measurement was performed using a texture analyzer (TA-XT plus,  
134 Stable Micro System, UK) equipped with an HDP/BSW probe. Briefly, after cooking  
135 loss determination, the samples were cooled at 4°C overnight, and each sample was  
136 cut into 6 to 8 cubes ( $1 \text{ cm}^2$  cross section) parallel to the orientation of muscle fiber  
137 and sheared by the texture analyzer. The average peak force of the subsamples was  
138 calculated and the shear force was expressed as N / $\text{cm}^2$ .

### 139 2.6 Muscle microstructure analysis

#### 140 2.6.1 Scanning electron microscope (SEM)

---

141 The meat samples in different stages of postmortem were dissected into  $2 \times 2 \times 3$   
142 mm parallel to the orientation of muscle fiber and fixed overnight in 2.5%  
143 glutaraldehyde, then rinsed for 1 h with distilled water and dehydrated with graded  
144 ethanol. Dried samples were sputter-coated with gold and observed with SEM  
145 (SU8010, Hitachi, Japan) at a magnification of  $500 \times$  (Qian et al., 2020).

#### 146 2.6.2 Transmission electron microscope (TEM)

147 The samples were cut into  $1 \times 1 \times 3$  mm and fixed overnight in 2.5%  
148 glutaraldehyde, then post-fixed with 1% OsO<sub>4</sub> and washed with 0.1 M phosphate  
149 buffer, followed by dehydration in ethanol. After embedded in spur resin, meat  
150 sections were prepared using the Leica ultramicrotome, and then stained with uranyl  
151 acetate and lead citrate and observed under TEM (H-7500, Hitachi, Japan) at a  
152 magnification of  $15,000 \times$  (Lang et al., 2016). The pictures were analyzed by using  
153 the software of Image-Pro Plus 6.0 (Media Cybernetics, USA).

#### 154 2.7. Statistical analysis

155 The data analyses were conducted using SPSS 25.0 (IBM, USA) and Origin  
156 2021b software (OriginLab, USA). The mean values of the variables were analysed  
157 by one-way ANOVA and Duncan-multiple range test, least significant differences ( $p <$   
158 0.05) were reported. The postmortem phases and cuts were considered as the fixed  
159 effects, and animals as the random effect. The principal component analysis (PCA) of  
160 the variables were done by the PCA package of Origin.

### 161 3. Results

#### 162 3.1 pH

---

163 As shown in Table 1, the pH of lamb oyster cut, short loin, knuckle and silverside  
164 declined from 6.50-6.58 in pre-rigor to 5.63-5.92 in rigor mortis ( $p<0.05$ ), and then  
165 remained stable from rigor mortis to post-rigor ( $p>0.05$ ). Short loin (5.63) and  
166 silverside (5.64) had lower ultimate pH than oyster cut (5.86) and knuckle (5.92) at 24  
167 h postmortem ( $p<0.05$ ).

### 168 3.2 Color

169 The  $L^*$ ,  $b^*$  and hue angle values were significantly higher in rigor mortis and  
170 post-rigor cuts than their pre-rigor counterparts ( $p<0.05$ , Table 1). Pre-rigor meat had  
171 lower  $a^*$  value than rigor mortis meat in the four cuts ( $p<0.05$ ), whereas pre-rigor and  
172 post-rigor meat had similar  $a^*$  value in short loin and silverside cuts ( $p>0.05$ ).

### 173 3.3 Water holding capacity (WHC)

174 As shown in Table 2, rigor mortis cuts had the highest thawing loss, followed by  
175 post-rigor cuts, whereas pre-rigor cuts had the lowest thawing loss ( $p<0.05$ ). The  
176 thawing loss of rigor mortis cuts (oyster cut, 4.02%; short loin, 8.21%; knuckle,  
177 3.18%; silverside, 6.14%) were almost twice as much as their pre-rigor counterparts  
178 (2.31%, 4.11%, 1.73% and 3.79%, respectively). Similarly, compare with rigor mortis  
179 cuts, pre-rigor cuts also had less total moisture loss ( $p<0.05$ ), there was no significant  
180 difference of cooking loss between pre-rigor and rigor mortis cuts ( $p>0.05$ ).

181 Pre-rigor cuts had higher NMR  $T_2$  relaxation time of immobilized water ( $T_{21}$ )  
182 compared with rigor mortis cuts ( $p<0.05$ ), and the  $T_{21}$  of pre-rigor short loin, knuckle  
183 and silverside were higher than those of post-rigor cuts ( $p<0.05$ ). The proton  
184 populations of immobilized water ( $P_{21}$ ) in short loin and silverside decreased by

---

185 0.26% and 0.79%, meanwhile, the proton population of free water ( $P_{22}$ ) in short loin  
186 increased by 0.51% during the onset of rigor mortis ( $p<0.05$ ).

### 187 3.4 Warner-Bratzler shear force (WBSF)

188 As shown in Figure. 1, WBSF values were higher in rigor mortis meat than in  
189 pre-rigor and post-rigor meat for all cuts except oyster cut ( $p<0.05$ ). For short loin,  
190 pre-rigor meat had lower WBSF than post-rigor meat (pre-rigor, 58.10 N; post-rigor,  
191 69.49 N;  $p<0.05$ ). However, for other cuts no different were found between pre-rigor  
192 and post-rigor meat ( $p>0.05$ ). Oyster cut had the lowest WBSF values than other cuts  
193 in different stages of postmortem ( $p<0.05$ ).

### 194 3.5 Micro- and ultra-structure

195 Micro- and ultra-structure of the lamb samples in the pre-rigor, rigor mortis and  
196 post-rigor phases are showed in Fig. 2 and 3. Compared to pre-rigor cuts, significant  
197 shrinkage of muscle fibers and the gaps formation among muscle fibers can be seen in  
198 rigor mortis and post-rigor cuts (Fig. 2). From pre-rigor to post-rigor, the diameters of  
199 muscle fiber of oyster cut, short loin, knuckle and silverside decreased from 33.30,  
200 37.60, 34.36 and 44.91  $\mu\text{m}$  to 29.34, 28.1, 27.24 and 30.64  $\mu\text{m}$ , respectively ( $p<0.05$ ,  
201 Fig. 4A). Pre-rigor cuts exhibited an intact structure and long sarcomere. During the  
202 onset of rigor mortis, the sarcomere shrank laterally and longitudinally (Fig. 3). Rigor  
203 mortis and post-rigor meat exhibited wide I-bands, dark A-bands, short sarcomeres  
204 and large inter-myofibrillar spaces. Degradation of Z-lines occurred in post-rigor cuts.  
205 From pre-rigor to post-rigor, the length of sarcomere of oyster cut, short loin, knuckle  
206 and silverside decreased from 1.57, 1.45, 1.52, 1.56  $\mu\text{m}$  to 1.37, 1.20, 1.34 and 1.30

---

207  $\mu\text{m}$ , respectively ( $p < 0.05$ , Fig. 4B).

### 208 3.6 Principal component analysis (PCA)

209 From the result of the PCA, 62.2% of the total variability was explained by the  
210 two first principal components (PCs) with 37.5% explained by PC1 and 24.7%  
211 explained by PC2. The PC1 was positively related with  $L^*$ ,  $b^*$  and hue angle, whereas  
212 negatively related with pH.  $T_{21}$  relaxation time constant had a strongly positive  
213 influence on PC2, whereas WBSF and thawing loss were negatively related to PC2.  
214 From the PCA score plot (Fig. 5B), there was a clear separation of pre-rigor cuts from  
215 rigor mortis and post-rigor cuts. Pre-rigor cuts were present in the negative side of  
216 PC1 characterized by higher pH and lower water loss, whereas rigor mortis and  
217 post-rigor sample were in the positive PC1 axis characterized by higher  $L^*$ ,  $b^*$  and  
218 water loss. The score plot highlighted that rigor mortis and post-rigor cuts had similar  
219 characteristics but different from pre-rigor cuts (Fig. 5B and Supplementary Fig. S1 to  
220 S4).

## 221 4. Discussion

### 222 4.1 Differential postmortem glycolysis in pre-rigor, rigor mortis and post-rigor result 223 in different meat quality

224 The conversion of muscle to meat during the postmortem period involves  
225 complex energy metabolism and biochemical reaction in pre-rigor, rigor mortis and  
226 post-rigor (Lawrie and Ledward, 2017; Pearce et al., 2011). Following exsanguination,  
227 the skeletal muscle lacks the oxygen supplied to produce ATP through oxidative  
228 metabolism. Glycolysis becomes the overarching pathway to produce ATP in the

---

229 postmortem period, and the accumulation of lactic acid causes pH decline and  
230 acidification of muscle (Lawrie and Ledward, 2017). Previous research studying in  
231 Poll Dorset cross-bred sheep (Ithurralde et al., 2018), Mongolian and Small-Tail Han  
232 crossbreed lamb (Xiao et al., 2020) and other lamb breeds (Geesink et al., 2011;  
233 Lawrie and Ledward, 2017) observed that the pH of lamb muscle declined from  
234 6.5-7.0 to 5.6-6.0 during the onset of rigor mortis, and then remained stable during  
235 subsequent aging process, which were in agreement with this study. The extent and  
236 rate of pH decline postmortem could affect the WHC and color of meat (Pearce et al.,  
237 2011). In the rigor mortis phase, the pH close to the isoelectric point of myofibrillar  
238 proteins and the net charges between myofibrillar proteins decrease to near zero,  
239 which results in the less ability of myofibrillar proteins to bind water molecules and  
240 the increase of free extra-myofibrillar water within muscle (Ijaz et al., 2020). The high  
241 level of free water could be associated with the increase of water loss and the decrease  
242 of WHC (Khan et al., 2019). Under a low pH, the denaturation of sarcoplasmic  
243 proteins, as well as the increase of free water could facilitate light scattering and  
244 reflectance, which could result in the high level of L\* values in rigor mortis and  
245 post-rigor cuts (Hughes et al., 2019; Ijaz et al., 2020). Dai et al. (2013) reported that  
246 the denaturation and precipitation of sarcoplasmic proteins to the myofibrils resulted  
247 in a decrease of WHC and an increase of lightness in pork *M. longissimus dorsi*  
248 muscle.

249 4.2 Various muscle contraction in pre-rigor, rigor mortis and post-rigor generate the  
250 variety of meat quality

---

251 Postmortem glycolysis and pH decline result in the longitudinal shortening of  
252 sarcomeres and lateral shrinkage of myofibrils (Ertbjerg and Puolanne, 2017; Hughes  
253 et al., 2019; Lana and Zolla, 2016). From pre-rigor to rigor mortis, the diameter of  
254 muscle fiber of oyster cut, short loin, knuckle and silverside decreased by 11.53%,  
255 23.32%, 23.25% and 36.45%, respectively; similarly, sarcomere length in those cuts  
256 decreased by 22.10%, 15.11%, 13.29% and 19.89%, respectively. The sarcomere  
257 length of ovine *longissimus thoracis et lumborum* and bovine *semitendinosus*  
258 decreased by 24.55% Wheeler et al. (1994) and 55.56% Stromer et al. (1967) during  
259 the onset of rigor mortis, which were in agreement with this study.

260 The structure of the muscle could affect the achromatic color of meat through  
261 affecting the extent of scattering, reflectance, transmission and absorption of light  
262 when the light passes through muscle fibers. The more scattering and reflection of  
263 light, meanwhile, the less absorption and transmission into the muscle structure  
264 contributing to pale meat (Hughes et al., 2019). In this study, L\* values increased  
265 gradually from pre-rigor to post-rigor. Rigor mortis and post-rigor cuts had higher L\*  
266 values than pre-rigor cuts. The increase of L\* could be related to transverse shrinkage  
267 of muscle fibers, extracellular space formation and light scattering increase (Ertbjerg  
268 and Puolanne, 2017; Hughes et al., 2019; Pearce et al., 2011). Offer and Cousins  
269 (1992) observed that the gaps between beef *sternomandibularis* muscle fibers formed  
270 and enlarged at 24 to 48 h postmortem, which was consistent with this study. Hughes  
271 et al. (2019) reported that the shrinkage of muscle fibers had a positive effect on the  
272 increase of light scattering. Ijaz et al. (2020) reported that the increase of L\* value in

---

273 beef *longissimus thoracis et lumborum* during postmortem storage period might  
274 attribute to the degradation of proteins by enzymes, which caused a weaken of protein  
275 structure and increased light dispersion. The increase of b\* and hue angle values from  
276 pre-rigor to post-rigor in this study could be due to myoglobin oxidation and  
277 metmyoglobin accumulation, which was associated with brown and unattractive color  
278 of meat (Jeong et al., 2009; Suman and Joseph, 2013). Post-rigor cuts had high level  
279 of b\* and hue angle values, which could cause a deviation of red hue and less  
280 desirable color of meat.

281 In this study, higher WBSF value was observed in rigor mortis cuts than in  
282 pre-rigor and post-rigor cuts. Sarcomere length is a critical indicator of meat  
283 tenderness, the decrease of sarcomere length leads to the increase of meat toughness  
284 (Chaosap et al., 2020). Wheeler et al. (1994) observed that the WBSF of ovine  
285 *longissimus thoracis et lumborum* increased from 5.1 kg at 3 h postmortem to 8.66 kg  
286 at 24 h postmortem, while the sarcomere length decreased from 2.24  $\mu\text{m}$  to 1.69  $\mu\text{m}$ .  
287 Xiao et al. (2020) reported that the WBSF values of roasted topsides of Mongolian  
288 and Small-Tail Han crossbreed lamb increased gradually from 8.74 kg to 11.38 kg  
289 during the onset of rigor mortis and then decreased to 4.58 kg at 7 d postmortem. The  
290 shrinkage of muscle fibers was related to higher amount of myofibrillar proteins and  
291 collagen per unit area of shear therefore tough meat (Fabre et al., 2018).

292 Rigor mortis cuts had higher total moisture loss than pre-rigor and post-rigor cuts,  
293 the thawing loss of rigor mortis cuts were almost twice as much as their pre-rigor  
294 counterparts in this study. The low level of WHC in rigor mortis cuts could associate

---

295 with the contraction of muscle during the postmortem period. The lateral shrinkage of  
296 myofibrils as the muscle entered rigor caused a decrease of myofilament lattice  
297 spacing (Huff-Lonergan and Lonergan, 2005). The decrease of space among the  
298 myofilaments results in an expulsion of water from intra-myofibrillar to  
299 extra-myofibrillar, where the water could be easily lost from meat (Ertbjerg et al.,  
300 2017; Ijaz et al., 2020; Pearce et al., 2011). However, the degradation of cytoskeletal  
301 proteins and swelling of the muscle cells during subsequent aging could improve  
302 WHC of post-rigor cuts (Hughes et al., 2014; Pearce et al., 2011).

303 4.3 Distinct water states in pre-rigor, rigor mortis and post-rigor result in different  
304 meat quality

305 The various distribution and mobility of myowater during the conversion of  
306 muscle to meat is a possible reason of the dissimilarities of the WHC in pre-rigor,  
307 rigor mortis and post-rigor cuts (Pearce et al., 2011). In this study, rigor mortis cuts  
308 had lower  $T_{21}$  relaxation time constant and WHC compared with pre-rigor and  
309 post-rigor cuts. The proton populations of immobilized water ( $P_{21}$ ) in rigor mortis  
310 oyster cut, short loin and silverside were lower than their pre-rigor and post-rigor  
311 counterparts, whereas the proton population of free water ( $P_{22}$ ) increased during the  
312 onset of rigor mortis. These results were in agreement with Wu et al. (2006) who  
313 reported that the decrease of  $T_{21}$  in pork *longissimus dorsi* muscle was associated with  
314 the shrinkage of myofibrils and the loss of water. Wu et al. (2007) reported a link  
315 between WHC and  $T_{21}$  in pork meat. The higher percentage of cooking loss, whereas  
316 lower  $T_{21}$  were observed in PSE (pale, soft, and exudative) meat than in normal and

---

317 DFD (dry, firm, and dark) meat. Transverse relaxation time constant of water proton  
318 associated with the interaction between water molecules and proteins or other  
319 macromolecules in the muscle structure. Lower  $T_2$  of proton suggests higher potential  
320 to reach a proton sink for the water molecules and lower mobility of water (Pearce et  
321 al., 2011; Shao et al., 2016). The partially shift of immobilized water to free water and  
322 repulsion from the intra-myofibrillar space to the extracellular space could be a  
323 possible reason for the low level of  $T_{21}$  and  $P_{21}$  of meat (Bertram et al., 2002; Khan et  
324 al., 2014; Wu et al., 2007). The increase of  $P_{22}$  indicates the increase of free  
325 extra-myofibrillar water in muscle (Pearce et al., 2011). It is hypothesized that the  
326 myowater volume in extra-myofibrillar space increased 1.6-fold during the onset of  
327 rigor mortis (Huff-Lonergan et al., 2005). The increase of the amount of free water  
328 within muscle resulted in an accumulation of water on the cut surface and lower WHC  
329 in rigor mortis meat than in pre-rigor meat (Devine et al., 2014).

## 330 5. Conclusion

331 Pre-rigor lamb meat had lower  $L^*$ ,  $b^*$ , hue angle and WBSF values, whereas  
332 higher water holding capacity than rigor mortis and post-rigor lamb meat. Oyster cut  
333 and knuckle had higher ultimate pH,  $L^*$  and water holding capacity than short loin  
334 and silverside. Distinct glycolysis, muscle contraction and water mobility could  
335 partially explain the differences of quality properties of lamb meat in different stages  
336 of postmortem. Therefore, pre-rigor lamb meat with short postmortem conditioning  
337 time had good tenderness, color and water holding capacity. The results of this study  
338 could provide some theoretical references for lamb meat sector to produce high

---

339 quality meat, meanwhile, to reduce cooler space and energy consumption and  
340 accelerate the turnover of meat.

341 **Declaration of Competing Interest**

342 The authors declare no conflicts of interest.

343 **Acknowledgements**

344 The authors thank the financial support from Agriculture Research System  
345 (CARS-38), Key Research and Development Plan Project of Hebei Province  
346 (19227121D), and National Agricultural Science and Technology Innovation Program  
347 (CAAS-ASTIP-2020-IFST) in China.

348

349

350

351

352

353

---

354 **References**

- 355 Bertram HC, Purslow PP, Andersen HJ. 2002. Relationship between meat Structure, water mobility,  
356 and distribution: A low-field nuclear magnetic resonance study. J Agric Food Chem 50:  
357 824-829.
- 358 Calnan H, Jacob RH, Pethick DW, Gardner GE. 2016. Production factors influence fresh lamb  
359 *longissimus* colour more than muscle traits such as myoglobin concentration and pH. Meat Sci  
360 119: 41-50.
- 361 Chaosap C, Sitthigripong R, Sivapirunthep P, Pungsuk A, Adeyemi K, Sazili AQ 2020. Myosin heavy  
362 chain isoforms expression, calpain system and quality characteristics of different muscles in  
363 goats. Food Chem 321: 126677.
- 364 Colle MJ, Richard RP, Killinger KM, Bohlscheid JC, Gray AR, Loucks WI, Doumit ME. 2016.  
365 Influence of extended aging on beef quality characteristics and sensory perception of steaks  
366 from the *biceps femoris* and *semimembranosus*. Meat Sci 119: 110-117.
- 367 Dai Y, Miao J, Yuan SZ, Liu Y, Li XM, Dai RT. 2013. Colour and sarcoplasmic protein evaluation of  
368 pork following water bath and ohmic cooking. Meat Sci 93: 898-905.
- 369 Devine C, Wells R, Lowe T, Waller J. 2014. Pre-rigor temperature and the relationship between lamb  
370 tenderisation, free water production, bound water and dry matter. Meat Sci 96: 321-326.
- 371 Ertbjerg P, Puolanne E. 2017. Muscle structure, sarcomere length and influences on meat quality: A  
372 review. Meat Sci 132: 139-152.
- 373 Fabre R, Dalzotto G, Perlo F, Bonato P, Teira G, Tisocco O. 2018. Cooking method effect on  
374 Warner-Bratzler shear force of different beef muscles. Meat Sci 138: 10-14.
- 375 Geesink G, Sujang S, Koohmaraie, M. 2011. Tenderness of pre- and post-rigor lamb *longissimus*

---

376 muscle. *Meat Sci* 88: 723-726.

377 Hopkins DL, Toohey ES, Warner RD, Kerr MJ, Ven R. 2010. Measuring the shear force of lamb meat  
378 cooked from frozen samples: comparison of two laboratories. *Anim Prod Sci* 50: 382-385.

379 Huff-Lonergan E, Lonergan SM. 2005. Mechanisms of water-holding capacity of meat: The role of  
380 postmortem biochemical and structural changes. *Meat Sci* 71: 194-204.

381 Hughes JM, Clarke FM, Purslow PP, Warner RD. 2019. Meat color is determined not only by  
382 chromatic heme pigments but also by the physical structure and achromatic light scattering  
383 properties of the muscle. *Compr Rev Food Sci Food Saf* 19: 44-63.

384 Hughes JM, Oiseth SK, Purslow PP, Warner RD. 2014. A structural approach to understanding the  
385 interactions between colour, water-holding capacity and tenderness. *Meat Sci* 98: 520-532.

386 Ijaz M, Li X, Zhang D, Hussain Z, Ren C, Bai Y, Zheng X. 2020. Association between meat color of  
387 DFD beef and other quality attributes. *Meat Sci* 161: 107954.

388 Ithurralde J, Bianchi G, Feed O, Nan F, Ballesteros F, Garibotto G, Bielli A. 2018. Variation in  
389 instrumental meat quality among 15 muscles from 14-month-old sheep and its relationship  
390 with fibre typing. *Anim Prod Sci* 58: 1358–1365

391 Jeong JY, Hur SJ, Yang HS, Moon SH, Hwang YH, Park GB, Joo ST. 2009. Discoloration  
392 characteristics of 3 major muscles from cattle during cold storage. *J Food Sci* 74: C1-C5.

393 Khan MA, Ali S, Abid M, Cao J, Jabbar S, Tume RK, Zhou G. 2014. Improved duck meat quality by  
394 application of high pressure and heat: A study of water mobility and compartmentalization,  
395 protein denaturation and textural properties. *Food Res Int* 62: 926-933.

396 Khan MA, Ali S, Yang H, Kamboh AA, Ahmad Z, Tume RK, Zhou G. 2019. Improvement of color,  
397 texture and food safety of ready-to-eat high pressure-heat treated duck breast. *Food Chem* 277:

---

398 646-654.

399 Kim Y, Ma D, Setyabrata D, Farouk M, Lonergan S, Huff-Lonergan E, Hunt M. 2018. Understanding  
400 postmortem biochemical processes and post-harvest aging factors to develop novel  
401 smart-aging strategies. *Meat Sci* 144: 74-90.

402 Lana A, Zolla L. 2016. Proteolysis in meat tenderization from the point of view of each single protein:  
403 A proteomic perspective. *J Proteomics* 147: 85-97.

404 Lang Y, Sha K, Zhang R, Xie P, Luo X, Sun B, Liu X. 2016. Effect of electrical stimulation and hot  
405 boning on the eating quality of Gannan yak *longissimus lumborum*. *Meat Sci* 112: 3-8.

406 Lawrie RA, Ledward DA. 2017. *Lawrie's Meat Science*. Woodhead, Abington, England. pp. 159-381.

407 Li C, Liu D, Zhou G, Xu X, Qi J, Shi P, Xia T. 2012. Meat quality and cooking attributes of thawed  
408 pork with different low field NMR T(21). *Meat Sci* 92: 79-83.

409 Li F, Yang Y, Jenna K, Xia C, Lv S, Wei W. 2018. Effect of heat stress on the behavioral and  
410 physiological patterns of Small-Tail Han sheep housed indoors. *Trop Anim Health Prod.* 50:  
411 1893-1901.

412 Li X, Zhang D, Ren C, Bai Y, Ijaz M, Hou C, Chen L. 2020. Effects of protein posttranslational  
413 modifications on meat quality: A review. *Compr Rev Food Sci Food Saf.*

414 Li Y, Li X, Wang J, Zhang C, Sun H, Wang C, Xie X. 2014. Effects of Oxidation on Water Distribution  
415 and Physicochemical Properties of Porcine Myofibrillar Protein Gel. *Food Biophysics* 9:  
416 169-178.

417 Nam KC, Jo C, Lee M. 2010. Meat products and consumption culture in the East. *Meat Sci* 86: 95-102.

418 Offer G, Cousins T. 1992. The mechanism of drip production: Formation of two compartments of  
419 extracellular space in muscle Post mortem. *J Sci Food Agric* 58: 107-116.

---

420 Pearce KL, Rosenvold K, Andersen HJ, Hopkins DL. 2011. Water distribution and mobility in meat  
421 during the conversion of muscle to meat and ageing and the impacts on fresh meat quality  
422 attributes: A review. *Meat Sci* 89: 111-124.

423 Qian S, Li X, Wang H, Wei X, Mehmood W, Zhang C, Blecker C. 2020. Contribution of calpain to  
424 protein degradation, variation in myowater properties and the water-holding capacity of pork  
425 during postmortem ageing. *Food Chem* 324: 126892.

426 Shao J, Deng Y, Song L, Batur A, Jia N, Liu D. 2016. Investigation the effects of protein hydration  
427 states on the mobility water and fat in meat batters by LF-NMR technique. *LWT - Food*  
428 *Science and Technology* 66: 1-6.

429 Stromer MH, Goll DE, Roth LE. 1967. Morphology of rigor-shortened Morphology of rigor-shortened.  
430 *J Cell Biol* 34: 431-445.

431 Sukumaran AT, Holtcamp AJ, Campbell YL, Burnett D, Schilling MW, Dinh TTN. 2018. Technological  
432 characteristics of pre- and post-rigor deboned beef mixtures from Holstein steers and quality  
433 attributes of cooked beef sausage. *Meat Sci* 145: 71-78.

434 Suleman R, Wang Z, Aadil RM, Hui T, Hopkins DL, Zhang D. 2020. Effect of cooking on the nutritive  
435 quality, sensory properties and safety of lamb meat: Current challenges and future prospects.  
436 *Meat Sci* 167: 108172.

437 Suman SP, Joseph P. 2013. Myoglobin chemistry and meat color. *Annu Rev Food Sci Technol* 4: 79-99.

438 Wheeler TL, Koohmaraie M. 1994. Prerigor and postrigor changes in tenderness of ovine longissimus  
439 muscle. *Anim Sci J* 72: 1232-1238.

440 Wu JY, Mills EW, Henning WR. 1995. Postmortem delay time and heating rate affect tenderness and  
441 ultrastructure of prerigor cooked bovine muscle. *J Food Sci* 60: 565-570.

---

442 Wu Z, Bertram HC, Böcker U, Ofstad R, Kohler A. 2007. Myowater dynamics and protein secondary  
443 structural changes as affected by heating rate in three pork qualities: A combined FT-IR  
444 microspectroscopic and <sup>1</sup>H NMR relaxometry study. *J Agric Food Chem* 55: 3990-3997.

445 Wu Z, Bertram HC, Kohler A, Böcker U, Ofstad R, Andersen HJ. 2006. Influence of aging and salting  
446 on protein secondary structures and water distribution in uncooked and cooked pork. A  
447 combined FT-IR microspectroscopy and <sup>1</sup>H NMR relaxometry study. *J Agric Food Chem* 54:  
448 8589-8597.

449 Xiao X, Hou C, Zhang D, Li X, Ren C, Ijaz M, Liu D. 2020. Effect of pre- and post-rigor on texture,  
450 flavor, heterocyclic aromatic amines and sensory evaluation of roasted lamb. *Meat Sci* 169:  
451 108220.

452

453

454

---

455 **Table legends**

456 **Table 1 pH and color values of lamb oyster cut, short loin, knuckle and silverside**  
457 **in the pre-rigor, rigor mortis and post-rigor phases.** Data were recorded as mean  
458  $\pm$  SD. A-C: Means with different letters indicate significant difference ( $p < 0.05$ )  
459 between postmortem phases in the same cut. a-c: Means with different letters indicate  
460 significant difference ( $p < 0.05$ ) between cuts in the same postmortem phase.

461

462 **Table 2 Thawing loss, cooking loss, total moisture loss, NMR T<sub>2</sub> relaxation times**  
463 **(T<sub>2b</sub>, T<sub>21</sub> and T<sub>22</sub>) and corresponding proton populations (P<sub>2b</sub>, P<sub>21</sub> and P<sub>22</sub>) of**  
464 **lamb oyster cut, short loin, knuckle and silverside in the pre-rigor, rigor mortis**  
465 **and post-rigor phases.** Data were recorded as mean  $\pm$  SD. A-C: Means with  
466 different letters indicate significant difference ( $p < 0.05$ ) between postmortem phases in  
467 the same cut. a-c: Means with different letters indicate significant difference ( $p < 0.05$ )  
468 between cuts in the same postmortem phase.

469

470

471

472

473  
474

**Table 1**

Parameters	Postmortem phases	Cuts			
		Oyster cut	Short loin	Knuckle	Silverside
pH	Pre-rigor	6.50±0.20 <sup>Aa</sup>	6.54±0.16 <sup>Aa</sup>	6.53±0.20 <sup>Aa</sup>	6.58±0.18 <sup>Aa</sup>
	Rigor mortis	5.86±0.13 <sup>Ba</sup>	5.63±0.10 <sup>Bb</sup>	5.92±0.17 <sup>Ba</sup>	5.64±0.07 <sup>Bb</sup>
	Post-rigor	5.96±0.27 <sup>Ba</sup>	5.63±0.11 <sup>Bb</sup>	5.88±0.17 <sup>Ba</sup>	5.69±0.13 <sup>Bb</sup>
CIE L*	Pre-rigor	31.60±1.74 <sup>Ca</sup>	28.01±1.28 <sup>Bc</sup>	30.1±1.56 <sup>Bb</sup>	27.57±1.52 <sup>Bc</sup>
	Rigor mortis	37.95±2.17 <sup>Ba</sup>	35.48±1.73 <sup>Ab</sup>	35.91±2.11 <sup>Ab</sup>	34.99±1.76 <sup>Ab</sup>
	Post-rigor	39.44±1.82 <sup>Aa</sup>	36.36±1.72 <sup>Abc</sup>	37.08±2.18 <sup>Ab</sup>	35.29±1.42 <sup>Ac</sup>
CIE a*	Pre-rigor	13.30±1.20 <sup>Ba</sup>	12.15±10.03 <sup>Bb</sup>	12.53±1.51 <sup>Bab</sup>	12.53±1.11 <sup>Bab</sup>
	Rigor mortis	14.78±10.09 <sup>Aa</sup>	13.17±0.95 <sup>Ab</sup>	14.79±1.33 <sup>Aa</sup>	14.20±1.33 <sup>Aa</sup>
	Post-rigor	14.81±1.32 <sup>Aa</sup>	12.5±0.94 <sup>ABb</sup>	14.67±1.80 <sup>Aa</sup>	12.31±0.85 <sup>Bb</sup>
CIE b*	Pre-rigor	2.20±0.51 <sup>Ca</sup>	1.77±0.41 <sup>Cb</sup>	1.94±0.51 <sup>Cab</sup>	1.91±0.39 <sup>Cab</sup>
	Rigor mortis	4.91±0.57 <sup>Bb</sup>	4.85±0.57 <sup>Bb</sup>	4.84±0.95 <sup>Bb</sup>	5.58±0.68 <sup>Ba</sup>
	Post-rigor	7.02±0.91 <sup>Aa</sup>	6.72±0.80 <sup>Aa</sup>	6.81±0.97 <sup>Aa</sup>	6.90±0.43 <sup>Aa</sup>
Hue angle	Pre-rigor	9.49±1.50 <sup>Ca</sup>	7.64±2.34 <sup>Cb</sup>	8.73±1.42 <sup>Cab</sup>	8.21±1.00 <sup>Cab</sup>
	Rigor mortis	18.31±1.80 <sup>Bb</sup>	21.64±1.73 <sup>Ba</sup>	16.90±1.64 <sup>Bc</sup>	21.29±1.90 <sup>Ba</sup>
	Post-rigor	26.53±2.31 <sup>Ab</sup>	29.19±1.84 <sup>Aa</sup>	23.19±2.07 <sup>Ac</sup>	29.15±1.85 <sup>Aa</sup>
Chroma	Pre-rigor	13.34±1.13 <sup>Ba</sup>	12.14±0.95 <sup>Bb</sup>	12.84±1.48 <sup>Cab</sup>	12.51±0.97 <sup>Cab</sup>
	Rigor mortis	15.51±0.97 <sup>Aa</sup>	13.88±1.44 <sup>Ab</sup>	15.46±1.46 <sup>Ba</sup>	15.42±1.31 <sup>Aa</sup>
	Post-rigor	15.75±1.12 <sup>Ab</sup>	13.83±1.23 <sup>Ac</sup>	16.95±1.60 <sup>Aa</sup>	14.18±0.99 <sup>Bc</sup>

475  
476  
477  
478  
479  
480  
481  
482  
483  
484  
485  
486  
487  
488  
489  
490  
491  
492  
493  
494  
495

496  
497

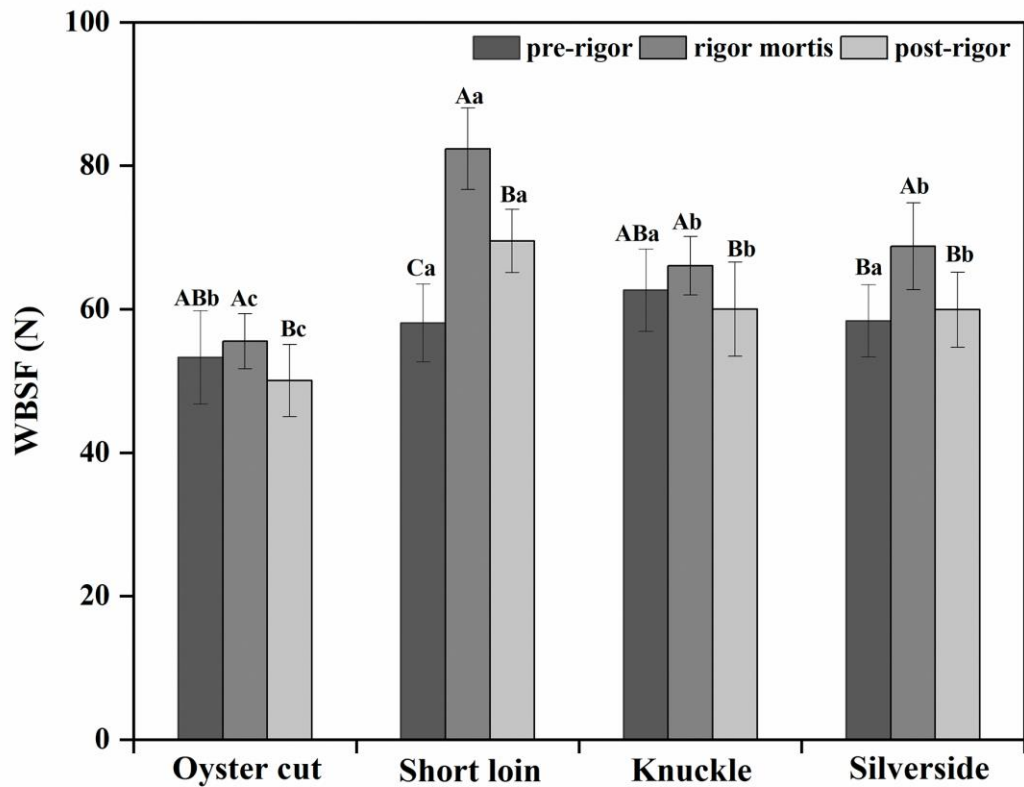
**Table 2**

Parameters	Postmortem phases	Cuts			
		Oyster cut	Short loin	Knuckle	Silverside
Thawing loss (%)	Pre-rigor	2.31±0.60 <sup>Bb</sup>	4.11±0.77 <sup>Ca</sup>	1.73±0.53 <sup>Bb</sup>	3.79±0.63 <sup>Ba</sup>
	Rigor mortis	4.02±0.56 <sup>Ac</sup>	8.21±0.91 <sup>Aa</sup>	3.18±0.74 <sup>Ad</sup>	6.14±0.87 <sup>Ab</sup>
	Post-rigor	2.18±0.66 <sup>Bc</sup>	5.91±1.44 <sup>Ba</sup>	2.11±0.79 <sup>Bc</sup>	4.36±0.85 <sup>Bb</sup>
Cooking loss (%)	Pre-rigor	28.93±1.86 <sup>Aa</sup>	27.28±1.27 <sup>Bb</sup>	28.98±2.00 <sup>Aa</sup>	27.4±2.34 <sup>Bb</sup>
	Rigor mortis	30.07±2.07 <sup>Aa</sup>	28.25±1.57 <sup>Bb</sup>	29.93±20.08 <sup>Aa</sup>	28.95±1.92 <sup>ABab</sup>
	Post-rigor	30.29±2.42 <sup>Aab</sup>	31.15±2.11 <sup>Aa</sup>	30.34±2.72 <sup>Aab</sup>	29.21±2.28 <sup>Ab</sup>
Total moisture loss (%)	Pre-rigor	32.04±2.07 <sup>Ba</sup>	31.75±2.21 <sup>Ba</sup>	30.88±2.56 <sup>Aa</sup>	30.68±2.60 <sup>Ca</sup>
	Rigor mortis	34.39±2.91 <sup>Ab</sup>	36.57±2.30 <sup>Aa</sup>	32.18±2.59 <sup>Ac</sup>	35.44±2.48 <sup>Aab</sup>
	Post-rigor	32.54±2.59 <sup>Bb</sup>	37.29±2.34 <sup>Aa</sup>	32.16±2.66 <sup>Ab</sup>	33.34±2.60 <sup>Bb</sup>
T <sub>2b</sub> (ms)	Pre-rigor	0.39±0.10 <sup>Bab</sup>	0.34±0.07 <sup>Abc</sup>	0.30±0.07 <sup>Bc</sup>	0.42±0.09 <sup>Aa</sup>
	Rigor mortis	0.50±0.15 <sup>Aa</sup>	0.38±0.12 <sup>Ab</sup>	0.43±0.18 <sup>Ab</sup>	0.36±0.10 <sup>Ab</sup>
	Post-rigor	0.46±0.09 <sup>ABa</sup>	0.37±0.11 <sup>Aa</sup>	0.37±0.10 <sup>ABa</sup>	0.46±0.19 <sup>Aa</sup>
T <sub>21</sub> (ms)	Pre-rigor	54.74±2.81 <sup>Aa</sup>	49.57±1.66 <sup>Ac</sup>	54.78±2.72 <sup>Aa</sup>	51.48±2.47 <sup>Ab</sup>
	Rigor mortis	50.60±2.95 <sup>Ba</sup>	44.8±2.79 <sup>Bc</sup>	50.72±1.63 <sup>Ba</sup>	47.64±2.45 <sup>Bb</sup>
	Post-rigor	54.06±3.13 <sup>Aa</sup>	46.17±2.96 <sup>Bd</sup>	51.60±2.72 <sup>Bb</sup>	49.46±1.98 <sup>Bc</sup>
T <sub>22</sub> (ms)	Pre-rigor	314.97±26.93 <sup>Ca</sup>	267.94±15.48 <sup>Ac</sup>	299.26±22.69 <sup>Bb</sup>	289.63±19.76 <sup>Ab</sup>
	Rigor mortis	336.17±21.13 <sup>Bb</sup>	276.25±19.75 <sup>Ad</sup>	365.59±45.68 <sup>Aa</sup>	302.19±12.88 <sup>Ac</sup>
	Post-rigor	366.2±27.49 <sup>Aa</sup>	271.92±22.34 <sup>Ac</sup>	361.19±26.80 <sup>Aa</sup>	299.81±22.27 <sup>Ab</sup>
P <sub>2b</sub> (%)	Pre-rigor	4.80±0.72 <sup>Ab</sup>	5.61±0.57 <sup>Aa</sup>	4.86±0.48 <sup>Ab</sup>	5.19±0.80 <sup>Aab</sup>
	Rigor mortis	4.09±0.51 <sup>Bb</sup>	5.14±0.89 <sup>Aa</sup>	4.44±0.65 <sup>ABb</sup>	5.04±0.90 <sup>Aa</sup>
	Post-rigor	4.00±0.34 <sup>Ba</sup>	4.18±1.41 <sup>Ba</sup>	4.08±0.62 <sup>Ba</sup>	4.22±0.84 <sup>Ba</sup>
P <sub>21</sub> (%)	Pre-rigor	93.23±0.69 <sup>Aa</sup>	92.23±0.47 <sup>Ab</sup>	92.94±0.83 <sup>Aa</sup>	92.83±0.81 <sup>Aa</sup>
	Rigor mortis	92.77±0.82 <sup>Aa</sup>	91.97±0.51 <sup>Bb</sup>	93.05±1.05 <sup>Aa</sup>	92.04±0.73 <sup>Bb</sup>
	Post-rigor	94.41±0.78 <sup>Aa</sup>	92.68±0.73 <sup>Ac</sup>	93.71±0.71 <sup>Ab</sup>	92.95±0.69 <sup>Ad</sup>
P <sub>22</sub> (%)	Pre-rigor	2.28±0.64 <sup>Aa</sup>	2.22±0.53 <sup>Ba</sup>	2.25±0.89 <sup>Aa</sup>	2.26±0.97 <sup>Aa</sup>
	Rigor mortis	2.39±0.77 <sup>Aa</sup>	2.73±0.72 <sup>Aa</sup>	2.38±10.01 <sup>Aa</sup>	2.58±0.90 <sup>Aa</sup>
	Post-rigor	1.44±0.38 <sup>Bb</sup>	1.95±0.52 <sup>Ba</sup>	1.76±0.79 <sup>Aab</sup>	2.15±0.61 <sup>Aa</sup>

498

499

500 **Figure legends**



501

502 **Fig. 1. Warner-Bratzler shear force (WBSF) values of lamb oyster cut, short loin,**

503 **knuckle and silverside in the pre-rigor, rigor mortis and post-rigor phases.** Data

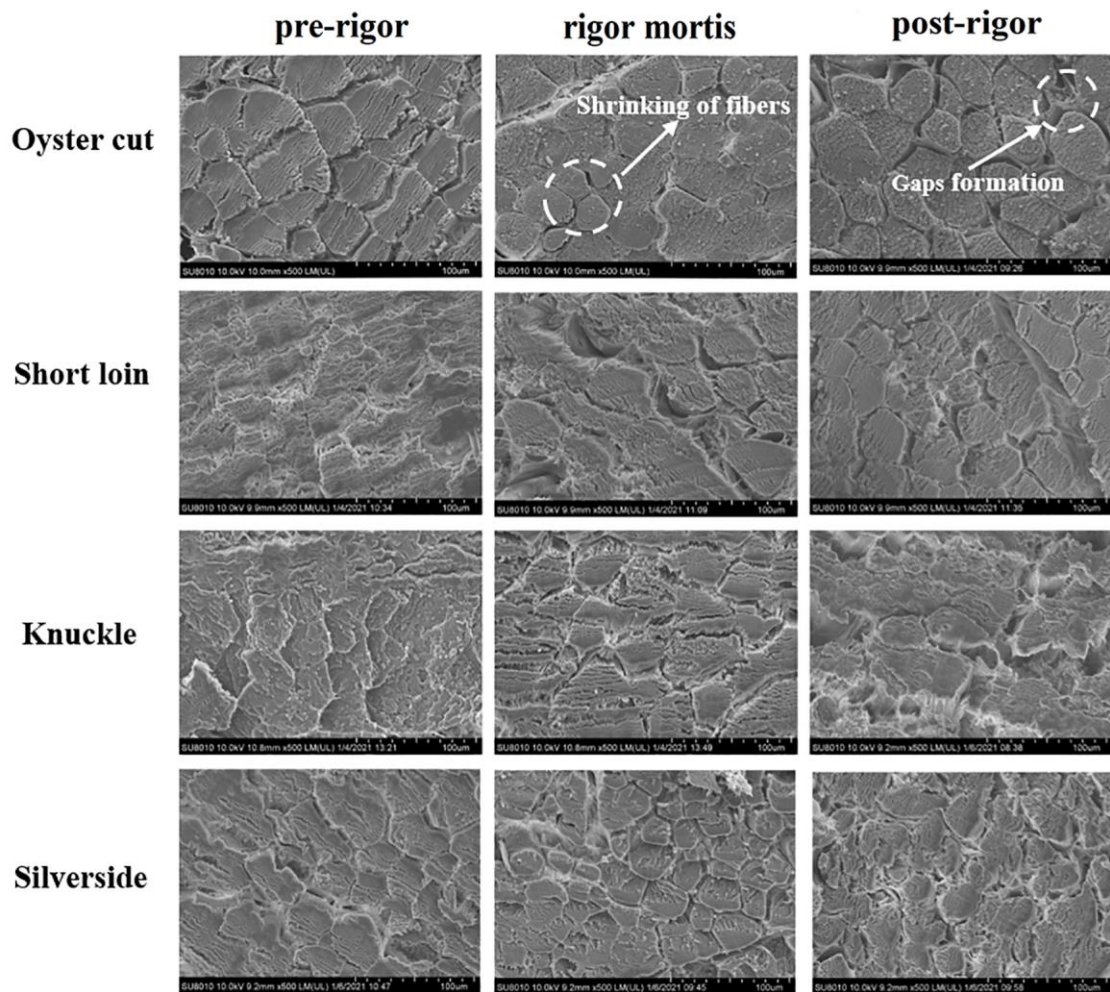
504 were recorded as mean  $\pm$  SD. A-C: Means with different letters indicate significant

505 difference ( $p < 0.05$ ) between postmortem phases in the same cut. a-c: Means with

506 different letters indicate significant difference ( $p < 0.05$ ) between cuts in the same

507 postmortem phase.

508



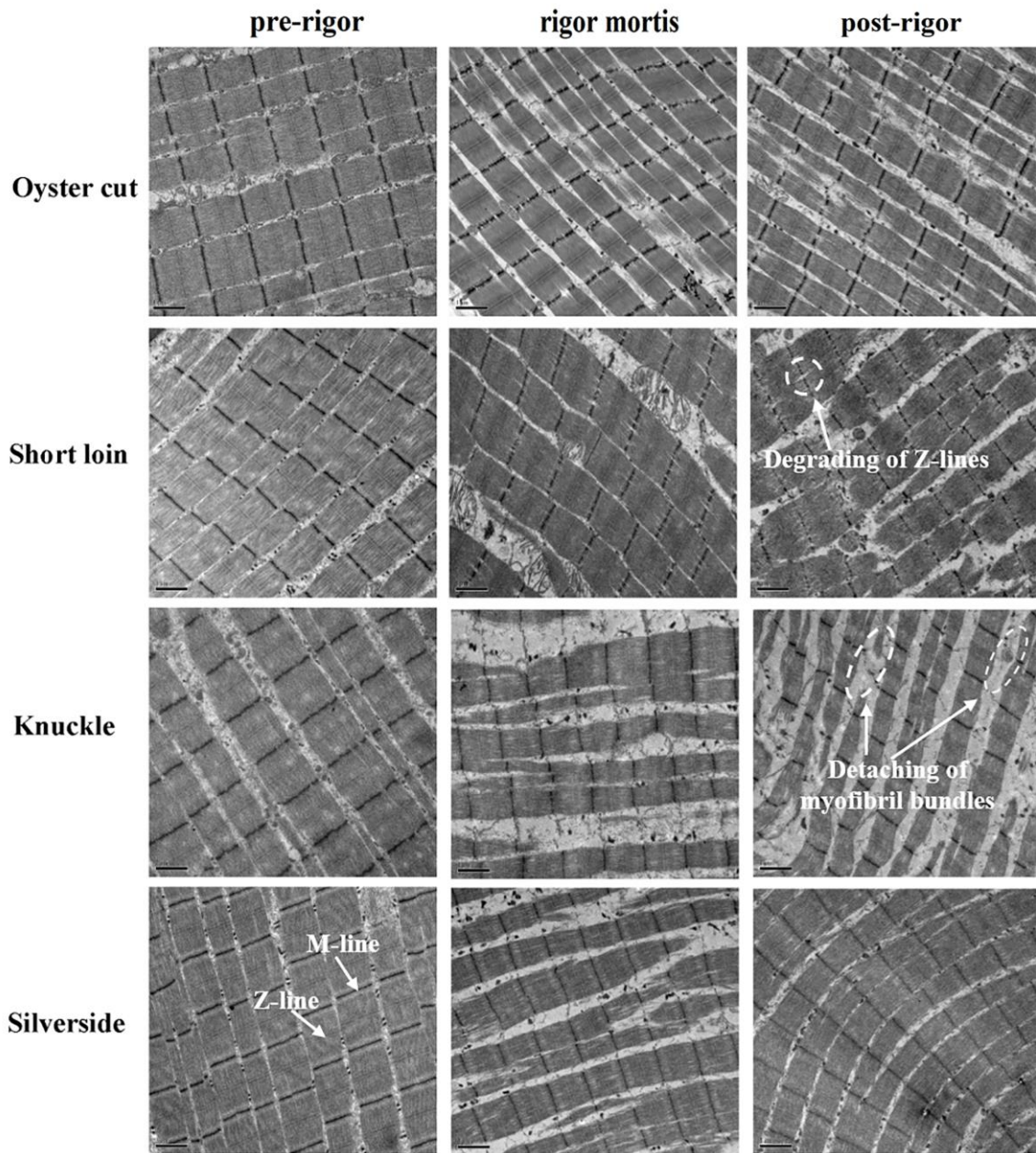
509

510 **Fig. 2. Scanning electron micrographs of lamb oyster cut, short loin, knuckle and**

511 **silverside in the pre-rigor, rigor mortis and post-rigor phases, (500 ×). Scale**

512 **bar=100 μm.**

513



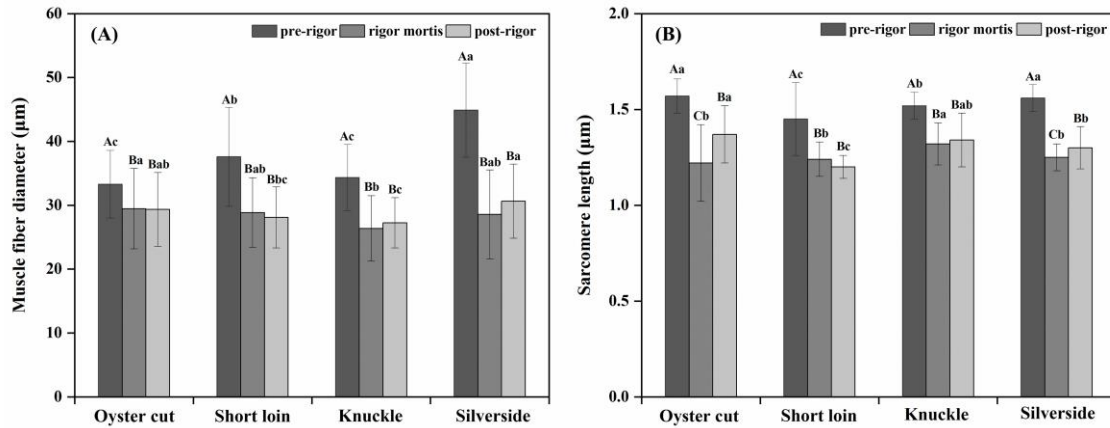
514

515 **Fig. 3. Transmission electron micrographs of lamb oyster cut, short loin, knuckle**

516 **and silverside in the pre-rigor, rigor mortis and post-rigor phases, (1,5000×).**

517 Scale bar=1 $\mu$ m.

518



519

520 **Fig. 4. Muscle fiber diameter and sarcomere length of lamb oyster cut, short loin,**

521 **knuckle and silverside in the pre-rigor, rigor mortis and post-rigor phases. A:**

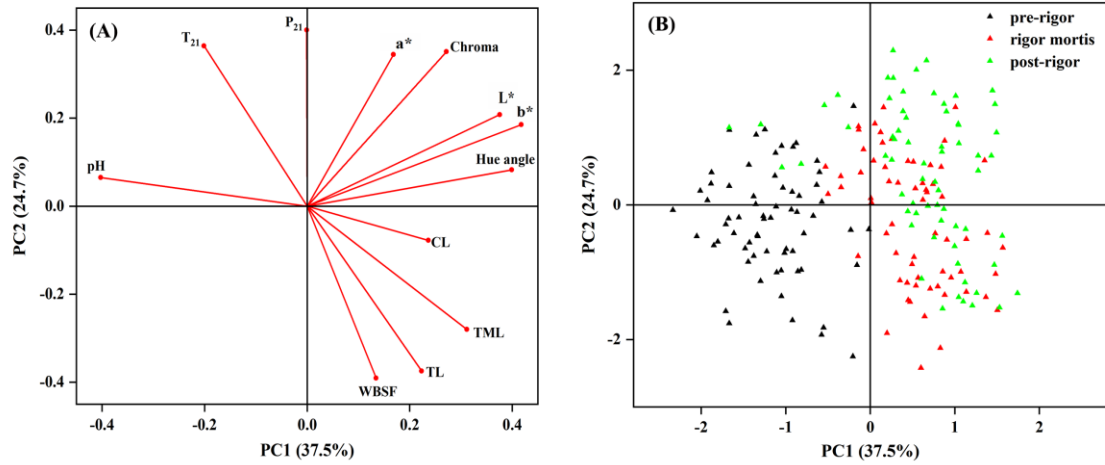
522 **muscle fiber diameter; B: sarcomere length. Data were recorded as mean  $\pm$  SD. A-C:**

523 **Means with different letters indicate significant difference ( $p < 0.05$ ) between**

524 **postmortem phases in the same cut. a-c: Means with different letters indicate**

525 **significant difference ( $p < 0.05$ ) between cuts in the same postmortem phase.**

526



527

528 **Fig. 5. Principal component analysis for meat quality parameters of lamb meat**

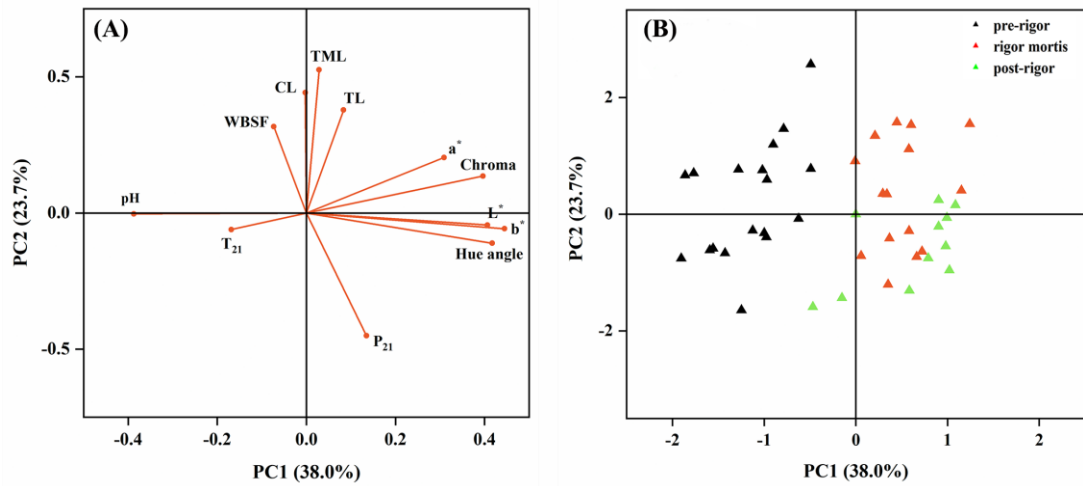
529 **in the pre-rigor, rigor mortis and post-rigor phases. A: loading plot; B: score plot.**

530 CL: cooking loss, TML: total moisture loss, TL: thawing loss.

531

532

## Supplementary Material



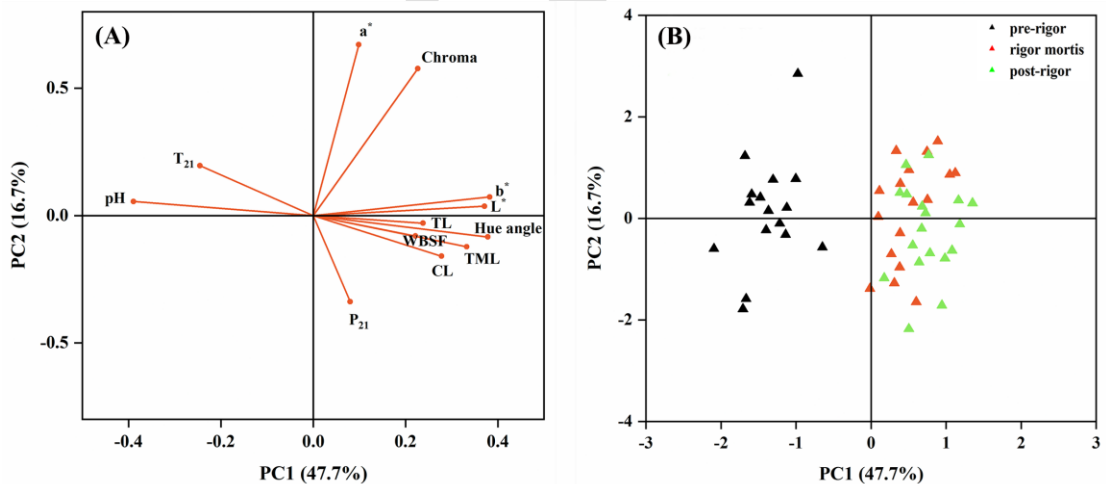
533

534 **S1 Principal component analysis for meat quality parameters of lamb oyster cut**

535 **in the pre-rigor, rigor mortis and post-rigor phases. A: loading plot; B: score plot.**

536 CL: cooking loss, TML: total moisture loss, TL: thawing loss.

537



538

539 **S2 Principal component analysis for meat quality parameters of lamb short loin**

540 **in the pre-rigor, rigor mortis and post-rigor phases. A: loading plot; B: score plot.**

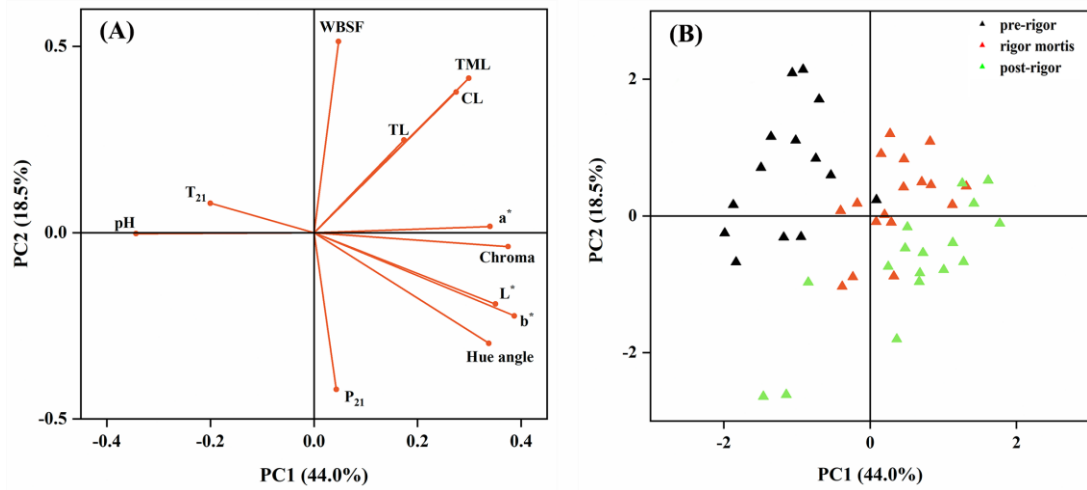
541 CL: cooking loss, TML: total moisture loss, TL: thawing loss.

542

543

544

545



546

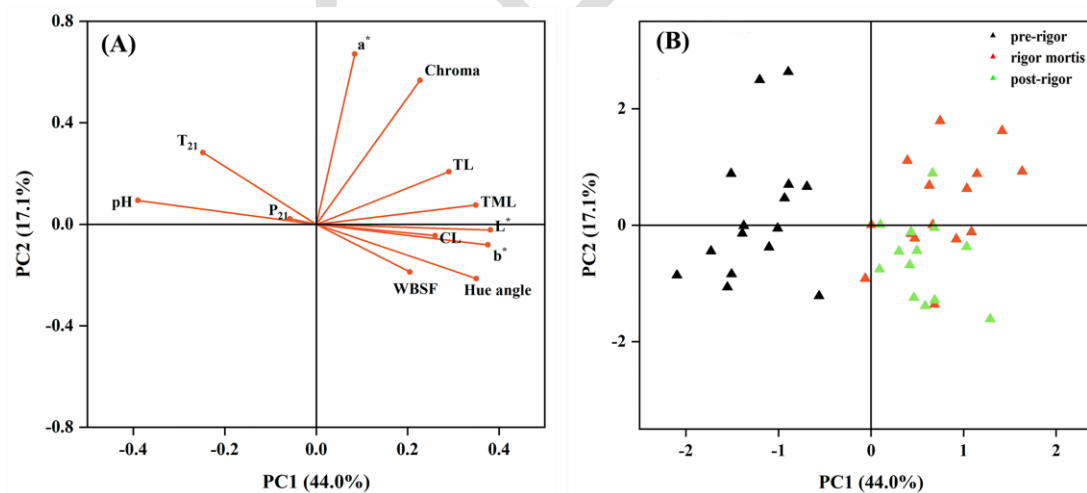
547

548 **S3 Principal component analysis for meat quality parameters of lamb knuckle in**  
549 **the pre-rigor, rigor mortis and post-rigor phases. A: loading plot; B: score plot. CL:**

550 **cooking loss, TML: total moisture loss, TL: thawing loss.**

551

552



553

554 **S4 Principal component analysis for meat quality parameters of lamb silverside**  
555 **in the pre-rigor, rigor mortis and post-rigor phases. A: loading plot; B: score plot.**

556 **CL: cooking loss, TML: total moisture loss, TL: thawing loss.**

557